N,N′-Diacetyl-*p*-phenylenediamine restores microglial phagocytosis and improves cognitive defects in Alzheimer's disease transgenic mice

Min Hee Park[a,b,c], Misun Lee[d,e], Geewoo Nam[e], Mingeun Kim[d], Juhye Kang[d], Byung Jo Choi[a,f], Min Seock Jeong[a,f], Kang Ho Park[a,b,c], Wan Hui Han[a,b,c], Eunyoung Tak[g,h], Min Sun Kim[g,h], Juri Lee[d], Yuxi Lin[i], Young-Ho Lee[i,j,k], Im-Sook Song[l], Min-Koo Choi[m], Joo-Yong Lee[g,h], Hee Kyung Jin[a,f,1], Jae-sung Bae[a,b,c,1], and Mi Hee Lim[d,1]

[a]Kyungpook National University Alzheimer's Disease Research Institute, Kyungpook National University, 41566 Daegu, Republic of Korea; [b]Department of Physiology, Cell and Matrix Research Institute, School of Medicine, Kyungpook National University, 41944 Daegu, Republic of Korea; [c]Department of Biomedical Science, BK21 Plus Kyungpook National University Biomedical Convergence Program, Kyungpook National University, 41944 Daegu, Republic of Korea; [d]Department of Chemistry, Korea Advanced Institute of Science and Technology, 34141 Daejeon, Republic of Korea; [e]Department of Chemistry, Ulsan National Institute of Science and Technology, 44919 Ulsan, Republic of Korea; [f]Department of Laboratory Animal Medicine, College of Veterinary Medicine, Kyungpook National University, 41566 Daegu, Republic of Korea; [g]Asan Institute for Life Sciences, Asan Medical Center, 05505 Seoul, Republic of Korea; [h]Department of Convergence Medicine, University of Ulsan College of Medicine, 05505 Seoul, Republic of Korea; [i]Protein Structure Group, Korea Basic Science Institute, Ochang, 28199 Cheongju, Chungbuk, Republic of Korea; [j]Neurovascular Research Group, Korea Brain Research Institute, 41068 Daegu, Republic of Korea; [k]Bio-Analytical Science, University of Science and Technology, 34113 Daejeon, Republic of Korea; [l]College of Pharmacy and Research Institute of Pharmaceutical Sciences, Kyungpook National University, 41566 Daegu, Republic of Korea; and [m]College of Pharmacy, Dankook University, 31116 Cheon-an, Republic of Korea

Edited by Li-Huei Tsai, Massachusetts Institute of Technology, Cambridge, MA, and accepted by Editorial Board Member Robert Desimone October 1, 2019 (received for review September 19, 2019)

As a central feature of neuroinflammation, microglial dysfunction has been increasingly considered a causative factor of neurodegeneration implicating an intertwined pathology with amyloidogenic proteins. Herein, we report the smallest synthetic molecule (*N,N′*-diacetyl-*p*-phenylenediamine [DAPPD]), simply composed of a benzene ring with 2 acetamide groups at the *para* position, known to date as a chemical reagent that is able to promote the phagocytic aptitude of microglia and subsequently ameliorate cognitive defects. Based on our mechanistic investigations in vitro and in vivo, 1) the capability of DAPPD to restore microglial phagocytosis is responsible for diminishing the accumulation of amyloid-β (Aβ) species and significantly improving cognitive function in the brains of 2 types of Alzheimer's disease (AD) transgenic mice, and 2) the rectification of microglial function by DAPPD is a result of its ability to suppress the expression of NLRP3 inflammasome-associated proteins through its impact on the NF-κB pathway. Overall, our in vitro and in vivo investigations on efficacies and molecular-level mechanisms demonstrate the ability of DAPPD to regulate microglial function, suppress neuroinflammation, foster cerebral Aβ clearance, and attenuate cognitive deficits in AD transgenic mouse models. Discovery of such antineuroinflammatory compounds signifies the potential in discovering effective therapeutic molecules against AD-associated neurodegeneration.

small molecule | antineuroinflammation | microglial phagocytosis | amyloid-β clearance | cognitive function

Neurodegeneration is defined as a progressive loss of neuronal structure and function (1). Increasing epidemiological evidence suggests that neuroinflammation, an innate immune mechanism of the central nervous system (CNS), is a major pathological contributor in neurodegeneration (2–5). Microglia play a key role in this process, as they are the resident phagocytes in the CNS responsible for identifying and eliminating pathogens (2, 6–12). Under normal conditions, the microglial immune response balances opposing roles in which they can either excrete proinflammatory mediators, involved in cellular recruitment and removal of impaired neurons, or produce antiinflammatory mediators, capable of promoting neuronal proliferation and synaptic plasticity (2, 10, 11). In contrast, the persistent presence of pathologic triggers (e.g., neuronal injury and protein aggregates) results in the chronic activation and impairment of microglia (2, 7). Microglial dysfunction is often characterized by 1) the elevated expression of neurotoxic proinflammatory mediators; 2) the decreased production of neurotrophic antiinflammatory mediators; and 3) the impaired ability to remove pathogens through the loss of phagocytic capacity (2, 7, 9, 10). The combined effects of such microglial anomalies incite negative neuronal consequences (10), amplified through self-propagation and positive-feedback loops (2, 7). Therefore, microglial dysfunction is a potential target for drug discovery and may offer a therapeutic opportunity against neurodegenerative diseases, including Alzheimer's disease (AD) (2, 7), Parkinson disease (3), and amyotrophic lateral sclerosis (4).

Significance

Microglial dysfunction accompanying the loss of phagocytic ability and the overexpression of neurotoxic factors presents a positive-feedback loop that contributes to the rapid progression of neurodegeneration. Termination of this cycle is considered a promising strategy to halt the progression of neurodegenerative diseases, including Alzheimer's disease; however, effective chemical reagents for this purpose have been very limited. Herein, we report a compact synthetic molecule capable of restoring microglial dysfunction and improving cognitive function. Our in-depth studies of such a molecular entity could be beneficial toward the urgent global search for a new and effective treatment of neurodegenerative disorders.

Author contributions: M.H.P., H.K.J., J.-s.B., and M.H.L. designed research; M.H.P., M.L., M.K., J.K., B.J.C., M.S.J., K.H.P., W.H.H., E.T., M.S.K., Y.L., Y.-H.L., I.-S.S., M.-K.C., J.-Y.L., H.K.J., and J.-s.B. performed research; M.L., M.K., and J.L. contributed new reagents/analytic tools; M.H.P., M.L., G.N., M.K., J.K., B.J.C., M.S.J., K.H.P., W.H.H., E.T., M.S.K., Y.L., Y.-H.L., I.-S.S., M.-K.C., J.-Y.L., H.K.J., J.-s.B., and M.H.L. analyzed data; and M.L., G.N., M.K., J.K., and M.H.L. wrote the paper.

The authors declare no competing interest.

This article is a PNAS Direct Submission. L.-H.T. is a guest editor invited by the Editorial Board.

Data deposition: All data discussed in the paper are included in *SI Appendix* and Movies S1–S8.

[1]To whom correspondence may be addressed. Email: hkjin@knu.ac.kr, jsbae@knu.ac.kr, or miheelim@kaist.ac.kr.

This article contains supporting information online at www.pnas.org/lookup/suppl/doi:10.1073/pnas.1916318116/-/DCSupplemental.

First published November 4, 2019.

AD is the most common form of dementia, accounting for approximately 47 million cases in 2016, and the number of AD patients is projected to reach almost 131 million by 2050 (13). The multifaceted etiopathology of AD involves a variety of pathological factors, such as neuroinflammation and amyloidogenic proteins, including amyloid-β (Aβ) (14). Moreover, the intertwined pathology between neuroinflammation and Aβ has been recognized to be critical toward the development of AD (7, 15). Loss of the phagocytic ability upon microglial dysfunction significantly decreases Aβ clearance, and the subsequent elevation of Aβ levels can induce microglial impairment through chronic activation (2, 9, 16). This malignant cycle is a strong driving force of neurodegeneration (17). Thus, the restoration of microglial function is able to reestablish neuronal homeostasis in AD.

Mounting research efforts have been dedicated to modulating microglial dysfunction with synthetic and repurposed chemical reagents (18–21). Among the candidates, a synthetic molecule, MCC950, exhibited the restorative efficacy toward microglial dysfunction as an inhibitor against NLRP3 (NACHT, LRR, and PYD domains-containing protein 3) inflammasome, promoting Aβ phagocytosis and improving cognitive function in vivo (22, 23). The aforementioned studies suggest that small molecules could be effective for regulating microglial dysfunction; however, practical working examples are exceedingly rare. We report the smallest synthetic molecular entity, *N*,*N*′-diacetyl-*p*-phenylenediamine (**DAPPD**), known to date as a neuroprotective compound capable of restoring cognitive defects to a significant extent by enhancing the microglial phagocytic clearance of Aβ species in the brains of AD transgenic mice (Fig. 1*A*). The structure of **DAPPD** is composed of a benzene ring only with 2 acetamide groups at the *para* position (Fig. 1*A*). Our mechanistic investigations indicate that **DAPPD** down-regulates the constituent proteins of NLRP3 inflammasome via the suppression of the NF-κB pathway and subsequently lowers the production of the proinflammatory mediators, caspase-1 and IL-1β, leading to the recovery of microglial function. Our overall studies substantiate the possibility of designing small and simple molecules for rectifying microglial dysfunction and boosting microglial phagocytic aptitude. The neuroprotective reagent, **DAPPD**, is a promising prototype of a remedial agent that can regulate neurodegenerative inflammation.

Results

Selection Rationale and Characterization of DAPPD. A small molecule, **DAPPD** (Fig. 1*A* and *SI Appendix*, Fig. S1), was selected as an antineuroinflammatory agent based on its molecular structure and previous research. A very recent study of the small molecule, benzene-1,4-diamine, demonstrated its in vivo efficacy to

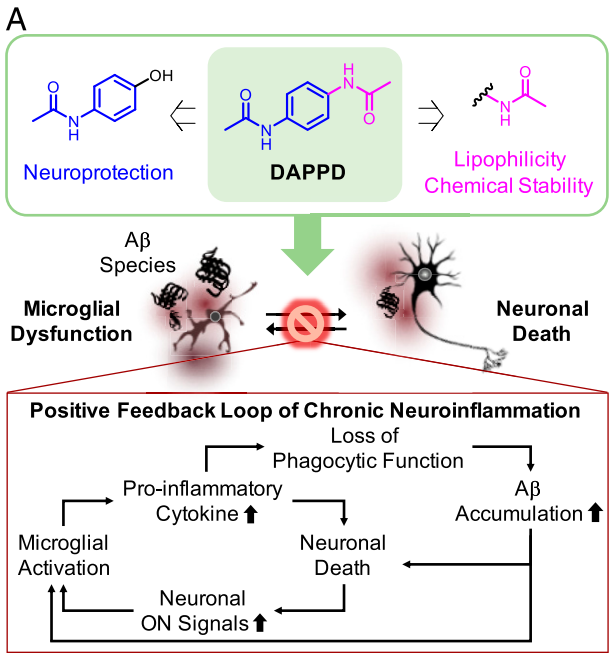

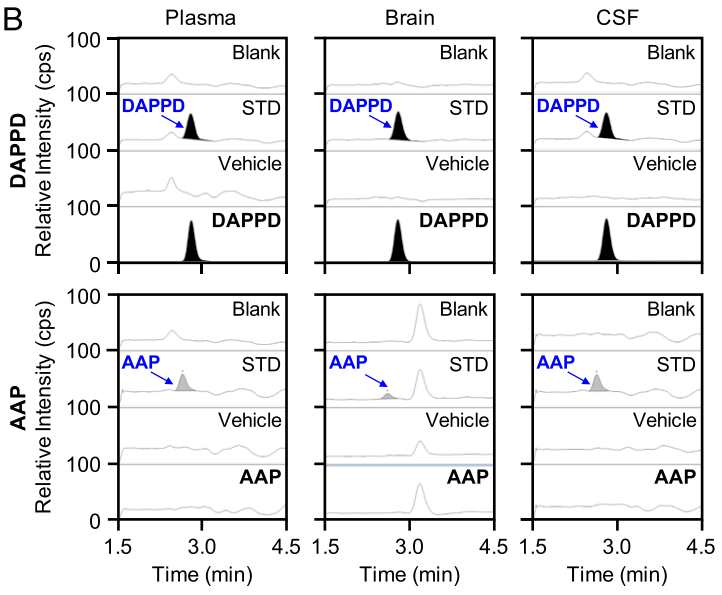

C

	$t_{1/2}$[e]	Cl_{int}[f]
DAPPD	> 60	3.9
Verapamil (Reference)	9.7	155

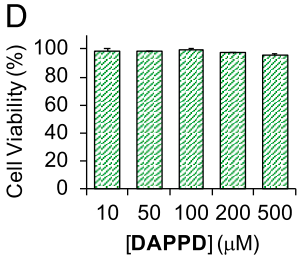

	Matrix	Concentration (ng/mL)[b]	SD[c]	CV (%)[d]
DAPPD	Plasma	6643	359	5.40
	Brain	409	309	75.6
	CSF	664	114	17.2
AAP	Plasma	n.d.	-	-
	Brain	n.d.	-	-
	CSF	n.d.	-	-

Fig. 1. Selection rationale and characterization of **DAPPD**. (*A*) Chemical structure and working principle of **DAPPD**. (*B*) Representative chromatograms and values from the brain-uptake studies[a] of **DAPPD** and acetaminophen (**AAP**) in the plasma, whole brain, and CSF 5 min after i.p. injection. [a]C57BL/6 mice; 10 mg/kg; i.p.; 5-min administration. [b]Mean (n = 3). [c]Standard deviation. [d]Coefficient of variation. n.d., not detected. (*C*) Metabolic stability; human liver microsomes. [e]Half-life ($t_{1/2}$). [f]Intrinsic clearance (Cl_{int}). (*D*) Cytotoxicity of **DAPPD**. Cell viability (%) of N2a neuroblastoma cells incubated with various concentrations of **DAPPD** for 24 h was measured by the 3-(4,5-dimethylthiazol-2-yl)-2,5-diphenyltetrazolium bromide assay (MTT assay). The cell viability (%) was calculated relative to cells treated with an equivalent amount of dimethyl sulfoxide (1% vol/vol). All error bars indicate SEM.

improve cognitive deficits in AD transgenic mice (24). In vitro experiments revealed that these effects of the molecule were associated with its modulative reactivity against metal-free Aβ and metal-bound Aβ. Aromatic amines are reported to induce hepatotoxicity and undergo acetylation by *N*-acetyltransferases in biological systems (25). As expected, metabolic studies in vivo revealed the formation of **DAPPD** upon administration of benzene-1,4-diamine, indicating the physiological significance of its chemical structure. The studies of **DAPPD**, herein, indicated that the molecule could noticeably improve cognitive defects in AD transgenic mice (vide infra). **DAPPD**, however, was not able to directly interact with metal-free Aβ or metal-bound Aβ and, as a result, showed no influence on their aggregation pathways (vide infra). Therefore, based on its structural similarity to acetaminophen (**AAP**) (Fig. 1*A*), an antipyretic and analgesic drug exhibiting mild antineuroinflammatory activity (26, 27), the antineuroinflammatory effects of **DAPPD** were investigated as shown in this study. The compact and symmetric structure of **DAPPD** presents its synthetic ease and ideal properties, including lipophilicity, which in turn promotes the molecule's ability to penetrate the blood–brain barrier (BBB) (28). The chemical structure of **DAPPD** is composed of a phenylacetamide and an additional acetamide moiety (Fig. 1*A*). The phenylacetamide structure of **DAPPD** can be found in **AAP**. Previous studies have indicated the neuroprotective effects of **AAP** stemming from its effect on the inflammatory pathways in lipopolysaccharide-induced cognitive impairment in mice (29). In addition, in the structure of **DAPPD**, the additional acetamide functionality could exhibit an improved enzymatic and metabolic stability under physiologically relevant conditions (30, 31). Taken together, **DAPPD** could be an ideal candidate as an antineuroinflammatory compound in vivo.

Prior to in vivo evaluation, **DAPPD**'s properties, such as metabolic stability, BBB permeability, and cytotoxicity, were evaluated for its biological applicability. Two distinct assays were performed to determine the molecule's 1) stability in plasma and 2) ability to bind to plasma proteins. First, **DAPPD** indicated notable stability in human plasma with 97% of the compound remaining after 120 min of incubation. Second, **DAPPD** exhibited significantly low plasma protein binding (0% bound, relative to 69 and 99% for dexamethasone and warfarin, respectively). These results suggest that **DAPPD** is stable in plasma and is relatively well distributed upon administration. Furthermore, the metabolic stability of **DAPPD** was investigated in vivo for identifying the possibility for its chemical transformation to **AAP**. To validate the brain accessibility and the metabolism of **DAPPD**, the compound (10 mg/kg) was intraperitoneally administered in C57BL/6 mice. Liquid chromatography–mass spectrometry analyses led to the detection of **DAPPD** in the plasma, cerebrospinal fluid (CSF), and brain after treatment of the compound, while **AAP** was not observed in these samples (Fig. 1*B*). These results confirm that **DAPPD** is able to cross the BBB without being metabolized to **AAP** in vivo. In addition, the oral administration of **DAPPD** (10 mg/kg) in vivo indicated its brain uptake (*SI Appendix*, Table S1). The in vitro metabolic studies of **DAPPD** using human liver microsomes revealed its moderate metabolic stability (half-life [$t_{1/2}$] > 60 min; intrinsic clearance [Cl_{int}] = 3.9; Fig. 1*C*). Moreover, the selectivity profiling of **DAPPD** was carried out against traditional pharmacological targets through the CEREP Safety-screen44 panel. The results from the screening (*SI Appendix*, Table S2) confirmed that **DAPPD** did not have notable activities (>50% inhibition) against the 44 targets tested. Lastly, no significant toxicity was observed in murine Neuro-2a (N2a) neuroblastoma cells treated with **DAPPD** at concentrations up to 500 μM (Fig. 1*D*). Together, **DAPPD** was identified to be suitable for in vivo assessment of its neuroprotective activity. Furthermore, the detailed mechanisms regarding **DAPPD**'s ability to attenuate microglial dysfunction under elevated neuroinflammatory conditions in AD transgenic mice were identified (vide infra).

Attenuation of Cognitive Deficits and Aβ Accumulation in DAPPD-Treated AD Transgenic Mice. In vivo efficacies of **DAPPD** were evaluated in 2 AD transgenic mice: 1) APP/PS1 mice, an AD double transgenic mouse model that contains both mutant amyloid precursor protein (APP) and presenilin-1 (PS1) transgenes, characterized by increased production and accumulation of Aβ aggregates as well as notable cognitive impairment (32); and 2) 5×FAD mice, an AD transgenic mouse model overexpressing mutant human APP695 (K670N/M671L [Swedish], I716V [Florida], and V717I [London]) and PS1 (M146L and L286V) that indicates the rapid onset of AD pathology and behavioral decline (33–35). Administration of **DAPPD** in the 2 AD transgenic mouse models took place in distinct manners with varying treatment periods and dosages. Based on preliminary experiments and the physiological characteristics of each model, APP/PS1 and 5×FAD mice underwent a 2- and 1-mo treatment period, respectively. More specifically, APP/PS1 mice show a less aggressive form of AD with a slower onset. Treatment of **DAPPD** in 7.5-mo-old APP/PS1 mice for 2 mo presents a potential prophylactic method against the progression and development of AD. On the other hand, the 5×FAD mouse model is a sensitive and fragile model of AD with the rapid development of severe AD pathology and cognitive dysfunction. Administrating 5×FAD mice with **DAPPD** for 1 mo indicates a potential therapeutic measure against a preexisting case of AD. The shorter administration interval applied to 5×FAD mice, compared to that of APP/PS1 mice, was a limitation in the study stemming from the fragility of this AD mouse model.

Wild-type (WT) and APP/PS1 mice (7.5 mo of age) were subject to intraperitoneal (i.p.) administration of **DAPPD** or vehicle at 2 mg/kg/day for 2 mo. After 30 d of treatment, the Morris Water Maze (MWM) test was performed to examine the spatial learning and memory of vehicle- or **DAPPD**-treated WT and APP/PS1 mice. As shown in Fig. 2 *A* and *B*, **DAPPD** did not affect the survival and the body weight of both WT and APP/PS1 mice during the treatment period. MWM tests demonstrated that the vehicle-treated APP/PS1 mice, relative to vehicle- and **DAPPD**-added WT mice, exhibited noticeably longer escape latencies and traveled longer distances to the platform. **DAPPD**-administrated APP/PS1 mice were able to locate the escape platform at earlier time points, and they traveled shorter distances to the platform in a manner comparable to those of WT mice. Such differences on escape latency and distance traveled were especially notable on the fifth and seventh days of training, at which point, the escape latencies of vehicle- and **DAPPD**-treated APP/PS1 mice deviated by approximately 2-fold (Fig. 2 *C*–*E*). In the probe trials conducted after 10 d of training, **DAPPD**-added APP/PS1 mice stayed in the target quadrant for longer periods than nontarget quadrants and traversed the target location more frequently compared to APP/PS1 mice injected with vehicle (Fig. 2 *F*–*H*). Interestingly, **DAPPD**-administrated APP/PS1 mice showed the similar results to WT mice. There were no notable differences in the distance traveled and swim speed of mice between the vehicle- or **DAPPD**-treated APP/PS1 mice in the probe trials (Fig. 2 *I* and *J*), indicating that **DAPPD** did not affect the motor function of APP/PS1 mice. These results suggest that **DAPPD** effectively improves the cognitive deficits in APP/PS1 mice.

Moving forward, to verify the effects of **DAPPD** on Aβ aggregate deposition, correlated to cognitive impairment in AD (36), the hippocampal and cortical accumulation of Aβ aggregates in the brains of APP/PS1 mice was monitored after a 2-mo period of compound administration. The deposition of Aβ plaques in APP/PS1 mice, detected by thioflavin-S (ThS) (37) and 6E10 (anti-Aβ antibody) (16), was reduced by approximately 6- and 2-fold, respectively, upon treatment of **DAPPD** relative to their vehicle-added counterparts (Fig. 2*K*).

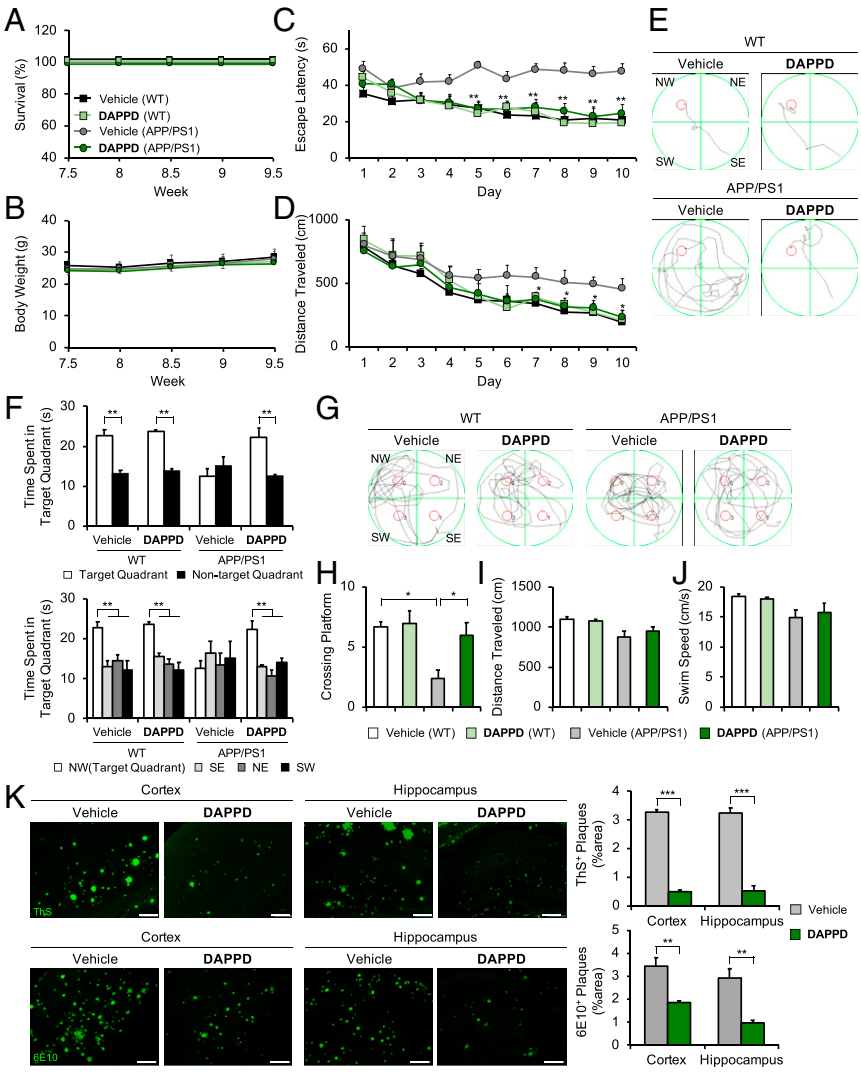

Fig. 2. In vivo efficacy of **DAPPD** in APP/PS1 mice. (*A* and *B*) Survival and body weight of vehicle- or **DAPPD**-treated WT and APP/PS1 mice during the treatment period. (*C* and *D*) Escape-latency time and distance traveled of each group in the MWM test. (*E*) Representative swimming paths on the 10th day of training. (*F* and *G*) Time spent in target platform and quadrants and representative swimming paths from the probe trials. (*H–J*) Number of times each animal entered the target zone (*H*), distance traveled (*I*), and swim speed (*J*) during the 60-s probe trial. (*K*) Analysis of the amounts of Aβ plaques, detected by ThS or 6E10, after the daily treatments of **DAPPD** for 2 mo (2 mg/kg/day; i.p.) in APP/PS1 mice starting at 7.5 mo of age. (Scale bars, 200 μm.) Animal number: *A*, *D*, *F*, and *H–J*: $n = 10$ per group; *K*, $n = 4$ per group. $^{*}P < 0.05$; $^{**}P < 0.01$; $^{***}P < 0.001$ by Student's *t* test or repeated-measures ANOVA, Tukey's post hoc test. All error bars indicate SEM.

The ability of **DAPPD** to restore cognitive function in AD transgenic mice was further confirmed employing 5×FAD mice. In a fashion similar to APP/PS1 mice, 3-mo-old 5×FAD mice treated with **DAPPD** for 1 mo (1 mg/kg/day; i.p.) exhibited enhanced spatial learning and memory in the MWM test (*SI Appendix*, Fig. S2 *A* and *B*). Moreover, the percentage area of 4G8-immunoreactive amyloid plaques was diminished in the brains of **DAPPD**-treated 5×FAD mice by approximately 40% compared to those of the vehicle-treated group (*SI Appendix*, Fig. S2*C*). In addition, the total, soluble, and insoluble levels of $A\beta_{40}$ were lowered by approximately 40, 20, and 50%, respectively (as for $A\beta_{42}$, approximately 30, 35, and 20% decreases were observed, respectively) (*SI Appendix*, Fig. S2*D*). Levels of soluble oligomeric Aβ, recognized as toxic Aβ species (38), were subject to a 30% reduction. The amount of congophilic amyloid plaques was also alleviated by 10%. Overall, our investigations with 2 AD transgenic mouse models demonstrate that **DAPPD** significantly improves cognitive defects and mitigates the accumulation of Aβ species.

Reduction of Neuroinflammation in APP/PS1 Mice upon Administration of DAPPD. To determine whether the antiinflammatory effects of **DAPPD** caused the decrease in the levels of Aβ species, microglia and astrocytes, the 2 major resident immune cells involved in the inflammatory response (2, 7), were histologically monitored using anti-Iba1 and anti-GFAP antibodies (16) in the brains of APP/PS1 mice (2 mg/kg/day, i.p.; 2 mo; 7.5 mo old). As shown in Fig. 3 *A* and *B*, the increased glial activation in APP/PS1 mice, induced by chronic neuroinflammation, was reduced by **DAPPD**. Activation of microglia in both the cortex and hippocampus was decreased by approximately 50% with the treatment of **DAPPD** compared to vehicle-added APP/PS1 mice. Note that the activation of astrocytes was lowered by approximately 30%. In addition, the expression of proinflammatory markers (i.e., *Tnf-α*, *Il-1β*, *Il-6*, and *iNos*) (16) and immunoregulatory cytokine (i.e., *Il-10*) (16), elevated in the cortices of vehicle-treated APP/PS1 mice, declined to levels comparable to those of WT mice upon administration of **DAPPD** in APP/PS1 mice (Fig. 3*C*). On the other hand, the

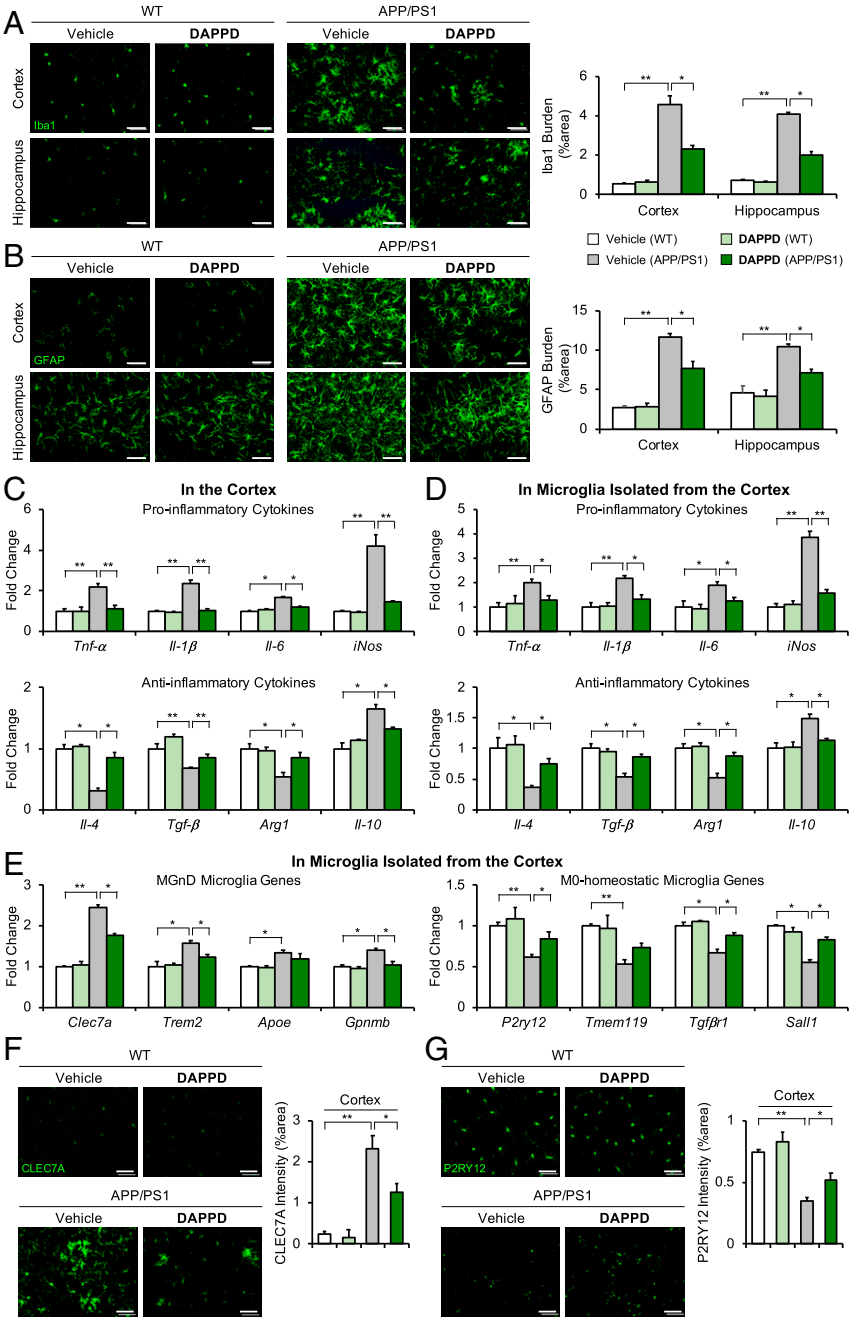

Fig. 3. Change in neuroinflammation upon treatment of **DAPPD** in WT and APP/PS1 mice. (*A* and *B*) Representative images and quantification of activated microglia (Iba1) and astrocyte (GFAP) from the cortices and hippocampi of the brains of vehicle- and **DAPPD**-treated WT and APP/PS1 mice. (Scale bars, 50 μm.) (*C* and *D*) Analysis of the alteration in mRNA levels of pro- and antiinflammatory cytokines in the cortices (*C*) and microglia isolated from the cortices (*D*) after administration of vehicle or **DAPPD** in WT and APP/PS1 mice. Proinflammatory marker: *Tnf-α*, *Il-1β*, *Il-6*, and *iNos*; immunoregulatory cytokine: *Il-10*; antiinflammatory marker: *Il-4*, *Tgf-β*, and *Arg1*. (*E*) Analysis of the changes in mRNA levels of MGnD microglia genes and M0-homeostatic microglia genes by treatment of vehicle or **DAPPD** to WT and APP/PS1 mice ($n = 4$ per group). (*F* and *G*) Representative images and quantification of CLEC7A and P2RY12 ($n = 4$ per group). (Scale bars, 50 μm.) Animal number: *A*–*G*, $n = 4$ per group. $^*P < 0.05$; $^{**}P < 0.01$ by one-way analysis of variance, Tukey's post hoc test. All error bars indicate SEM.

amounts of antiinflammatory markers (i.e., *Il-4*, *Tgf-β*, and *Arg1*) (16), down-regulated in APP/PS1 mice introduced with vehicle, were enhanced in the **DAPPD**-treated group. Therefore, our histological and biochemical experiments support that **DAPPD** is able to lower the chronic activation of microglia and astrocytes under neuroinflammatory conditions.

Antineuroinflammatory Effects of DAPPD Originated from Microglia. In the brain, diverse types of cells are associated in the inflammation process (2, 7). During the immune mechanism, the signaling molecules (e.g., cytokines) released from cells play a role in intercellular communication and controlling the inflammation process (2, 7, 10). To identify the cellular source of **DAPPD**'s antiinflammatory activity in the brain, we cultured 3 types of primary murine brain cells (i.e., microglia, astrocytes, and neurons). We first determined the toxicity of **DAPPD** against these cells by the 2-(4-iodophenyl)-3-(4-nitrophenyl)-5-(2,4-disulfophenyl)-2*H*-tetrazolium (WST-1) and terminal deoxynucleotidyl transferase

dUTP nick end labeling (TUNEL) assays. **DAPPD** did not exhibit its notable cytotoxicity or induce apoptosis in the abovementioned cell types (*SI Appendix*, Fig. S3 *A* and *B*). Next, Aβ-induced alterations in the in vitro expression of inflammatory markers were examined in these cells with and without the treatment of **DAPPD** (*SI Appendix*, Fig. S3*C*). The conditioned media (CM) containing a secreted mixture of diverse signaling mediators (39) from these 3 types of cells were collected and treated to either astrocytes (CM from microglia) or microglia (CM from astrocytes or neurons). In the presence of $A\beta_{42}$ (*SI Appendix*, Fig. S3*D*), microglia exhibited elevated levels of proinflammatory markers (i.e., *Tnf-α*, *Il-1β*, *Il-6*, and *iNos*) (16) and immunoregulatory cytokine (i.e., *Il-10*) (16), as well as reduced amounts of antiinflammatory markers (i.e., *Il-4*, *Tgf-β*, and *Arg1*) (16), relative to the control (i.e., microglia without $A\beta_{42}$ incubation). The concurrent introduction of **DAPPD** and $A\beta_{42}$ to microglia could noticeably restore the expression of inflammatory markers to the levels comparable to those of the control (*SI Appendix*, Fig. S3*D*), indicating that **DAPPD** mitigated the Aβ-mediated inflammatory response in microglia. The CM from Aβ-treated microglia triggered an inflammatory response in astrocytes, evidenced by the changes in the expression of inflammatory markers (*SI Appendix*, Fig. S3*E*). Astrocytes incubated in the CM from **DAPPD**-treated microglia expressed inflammatory markers at the levels comparable to those of the astrocytes incubated with the CM from the control group.

In contrast, the direct treatment of **DAPPD** did not abate the Aβ-triggered inflammatory response in astrocytes (*SI Appendix*, Fig. S3*F*). The CM from astrocytes incubated with $A\beta_{42}$ and **DAPPD** induced an inflammatory response in microglia (*SI Appendix*, Fig. S3*G*), suggesting that **DAPPD** could not divert the astrocyte-mediated modulation of inflammatory signaling in microglia. Moreover, **DAPPD** could not prevent Aβ-induced changes in the expression of neuronal "off" signals (i.e., *Bdnf*, *Cd47*, and *Cd200*) and a majority of the "on" signals (i.e., *Cxcl10* and *Ccl21*) (*SI Appendix*, Fig. S3*H*), responsible for sustaining the resting state and eliciting the activation of microglia, respectively (16, 40). Similar to the CM from Aβ-treated neurons, the CM from **DAPPD**-added neurons provoked an inflammatory response in microglia (*SI Appendix*, Fig. S3*I*). Together, these observations indicate that **DAPPD** is capable of directly diminishing the Aβ-induced inflammatory response of microglia among the 3 types of cells tested in this study. Moreover, through indirect effects prompted by microglia, **DAPPD** may be able to prevent the secondary inflammatory response, a propagated reaction resulting from the microglial secretion of inflammatory markers, in astrocytes. To identify the changes of microglia-specific inflammatory cytokines at the cellular level, we confirmed the expression of pro- and antiinflammatory cytokines in microglia isolated from the cortices of WT and APP/PS1 mice with and without treatment of **DAPPD**. These results (Fig. 3*D*) were consistent with the histological analysis of the cortices (Fig. 3*C*). Thus, the antiinflammatory effects of **DAPPD** could stem from its direct influence against microglia, responsible for the propagation of inflammatory signaling.

Microglia present a homeostatic functional signature expressing M0-homeostatic microglia genes, such as *P2ry12*, *Tmem119*, *Tgfβr1*, and *Sall1*, in the healthy brain. During the course of neurodegeneration, microglia lose their homeostatic molecular signature and exhibit a disease-associated phenotype by up-regulating inflammatory molecules, including *Clec7a*, *Trem2*, *Apoe*, and *Gpnmb* (MGnD microglia genes) (41–45). Based on previous studies, we investigated the mRNA levels of M0-homeostatic microglia genes and MGnD microglia genes in WT or APP/PS1 mice with or without administration of **DAPPD**. *Clec7a*, *Trem2*, *Apoe*, and *Gpnmb* were up-regulated in microglia derived from the cortices of vehicle-treated APP/PS1 mice, compared to those of vehicle-treated WT mice. Levels of these genes were reduced in **DAPPD**-administrated APP/PS1 mice relative to the vehicle-treated APP/PS1 mice (Fig. 3*E*). Moreover, the expression of M0-homeostatic microglial genes, down-regulated in the APP/PS1 mice relative to WT mice, was noticeably increased by treatment of **DAPPD** (Fig. 3*E*). Our immunofluorescence experiments demonstrated that the protein levels of CLEC7A and P2RY12A, up-regulated and down-regulated in APP/PS1 mice, respectively, underwent noticeable reductions and augmentations in **DAPPD**-treated APP/PS1 mice, compared to vehicle-added APP/PS1 mice (Fig. 3 *F* and *G*). These results support that **DAPPD** attenuates neuroinflammation by regulating functional phenotypes of microglia in APP/PS1 mice.

Promotion of Phagocytic Capacity of Microglia under Chronic Neuroinflammation by DAPPD. The phagocytic capability of microglia poses an important aspect of the inflammatory response against external stimuli, such as Aβ, the persistent presence of which can induce chronic microglial activation (2, 7). With confirmation that the antiinflammatory activity of the molecule originates from microglia (*SI Appendix*, Fig. S3), the influence of **DAPPD** toward microglial phagocytosis, defective under AD-related pathological conditions (7, 16), was analyzed in vivo using confocal microscopy. Volumetric quantification of the overlapping fluorescence regions through 3-dimensional reconstruction conferred a numerical representation of the microglial phagocytic process.

Images of the brain slices coimmunostained with anti-Iba1 and 6E10 antibodies (16) or anti-Iba1 antibody and ThS (37) showed that Aβ-associated microglial recruitment was increased in **DAPPD**-treated APP/PS1 mice (2 mg/kg/day, i.p.; 2 mo; 7.5 mo old), compared to vehicle-added APP/PS1 mice (Fig. 4*A* and *SI Appendix*, Fig. S4*A*). To examine the phagocytic aptitude of microglia more closely, Lamp1, a membrane protein expressed in microglial lysosomes (16, 46), was monitored, along with $Iba1^+$/$6E10^+$ or $Iba1^+$/ThS^+ amyloid plaques. Overlaying regions of the 3 fluorescence images presented that the volumes of microglial phagolysosomes, Aβ-associated phagolysosomes, and microglia occupied by Aβ-loaded phagolysosomes were increased by approximately 2.8-, 1.3-, and 2.3-fold, respectively, in **DAPPD**-administrated APP/PS1 mice relative to those in vehicle-treated APP/PS1 mice (Fig. 4*B* and *SI Appendix*, Fig. S4*B*).

Additionally, the morphology of microglia, closely related to its function (16, 47), was analyzed to confirm the effects of **DAPPD** on the phagocytic function of microglia. The amoeboid morphology of Aβ-associated microglia in **DAPPD**-treated APP/PS1 mice indicated that the compound could enhance the microglial phagocytosis of Aβ (Fig. 4*C* and *SI Appendix*, Fig. S4*C*). Quantification of the morphological parameters confirmed the transition of **DAPPD**-incubated microglia toward its phagocytic state (16). Treatment of **DAPPD** decreased microglial volume, dendrite length, as well as the number of segments, terminal points, and branch points and increased cell body size (Fig. 4 *C*, *Right* and *SI Appendix*, Fig. S4 *C*, *Right*). Lastly, **DAPPD**-administrated APP/PS1 mice exhibited the increased levels of smaller Aβ species (<25 μm) and decreased the amounts of larger Aβ aggregates (25–50 μm, >50 μm), compared to those of the vehicle-treated APP/PS1 mice (Fig. 4*D* and *SI Appendix*, Fig. S4*D*). Therefore, it can be inferred that the enhanced phagocytic capacity of **DAPPD**-treated microglia led to the enhancement in the degradation of larger Aβ species. Overall, our immunohistological studies demonstrate that **DAPPD** can restore the phagocytic activity of microglia, defective in APP/PS1 mice (16, 48), as evidenced by the increased colocalization of Aβ plaques and lysosomes within microglia, the shifts in microglial morphology, and the changes in the size distribution of Aβ aggregates.

DAPPD-Induced Down-Regulation of the NLRP3 Inflammasome Proteins through the Suppression of the NF-κB Pathway. The NLRP3 inflammasome is a signaling mediator composed of

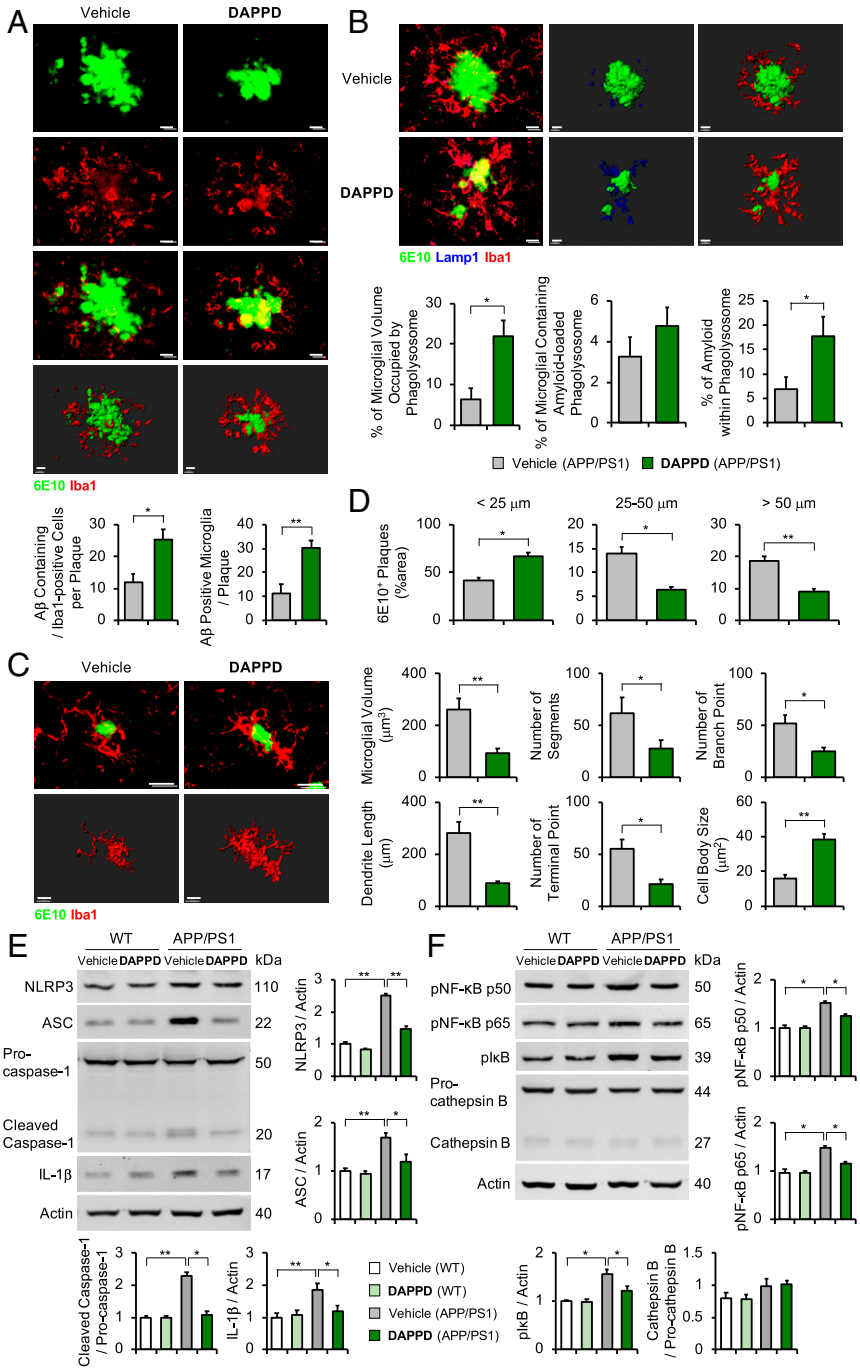

Fig. 4. Effects of **DAPPD** toward the microglial phagocytosis of Aβ and the expression of NLRP3 inflammasome-related proteins mediated by the NF-κB or cathepsin B pathways. (*A*) Immunostaining images of the colocalization of microglia (Iba1, red) with Aβ aggregates (6E10, green) and quantification of Aβ positive cells and microglia. (Scale bars, 10 μm.) (*B*) Immunofluorescence images of Aβ aggregates (6E10, green) encapsulated within phagolysosomes (Lamp1, blue) in microglia (Iba1, red) from the brains of vehicle- or **DAPPD**-treated APP/PS1 mice. Quantification of the microglial volume occupied by Lamp1$^+$ phagolysosomes, percentage of the microglia containing Aβ-loaded phagolysosome, and Aβ encapsulated in phagolysosomes. (Low magnification: scale bars, 10 μm; high magnification: scale bars, 10 μm.) (*C*) Morphology of microglia (Iba1, red) surrounded by Aβ (6E10, green) in the cortices of vehicle- or **DAPPD**-treated APP/PS1 mice. (Scale bars, 10 μm.) Three-dimensional reconstruction from confocal image stacks. (*D*) Morphometric analysis of Aβ plaques in vehicle- or **DAPPD**-treated APP/PS1 mice. (*E* and *F*) Effects of **DAPPD** on the expression of the proteins related to NLRP3 inflammasome, NF-κB signaling, and cathepsin B in the cortices of WT and APP/PS1 mice. Animal number: *A–F*, $n = 4$ per group. Three-dimensional reconstruction from confocal image stacks for *A–C*. *$P <$ 0.05; **$P < 0.01$ by one-way analysis of variance, Tukey's post hoc test. All error bars indicate SEM.

NLRP3, ASC (apoptosis-associated speck-like protein containing CARD), and procaspase-1 (22, 49). The activated NLRP3 inflammasome is responsible for cleaving procaspase-1 to produce caspase-1, which subsequently promotes the maturation of IL-1β, a representative proinflammatory cytokine (49). Recent studies have demonstrated NLRP3 inflammasome's association with Aβ-induced inflammation. Moreover, the expression of NLRP3 in microglia reportedly affected the cerebral Aβ deposition and cognitive function in AD transgenic mice (49). Thus, the regulation of NLRP3 inflammasome formation in

microglia has received attention as a promising strategy to diminish neuroinflammation in AD (22, 49).

To comprehend **DAPPD**'s antiinflammatory activity, its influence on the expression of NLRP3 inflammasome-associated proteins, i.e., NLRP3, ASC, and IL-1β, in APP/PS1 mice was investigated by gel electrophoresis with Western blotting (gel/Western blot). As presented in Fig. 4*E*, **DAPPD** down-regulated the production of NLRP3, ASC, and IL-1β. Moreover, a notable decrease in the ratio of cleaved caspase-1 to procaspase-1 was observed upon treatment of **DAPPD**. These results suggest that the suppressed generation of NLRP3 and ASC by **DAPPD** may reduce the activation of caspase-1 and, consequently, IL-1β. Note that no noticeable direct interaction between **DAPPD** and NLRP3 was observed, monitored by nuclear magnetic resonance spectroscopy (*SI Appendix*, Fig. S5).

A major upstream process involved in NLRP3 inflammasome formation is the NF-κB pathway (50). Previous studies reported that the activation of NF-κB signaling could induce the up-regulation of NLRP3, leading to an increase in the level of NLRP3 inflammasome (51). NF-κB is a protein complex composed of the P50 and P65 dimer that is involved in cell survival, inflammation, and immune response (52). Under normal conditions, the NF-κB dimer is inactive and retained in the cytoplasm by binding to specific inhibitor proteins known as IκB (53). When NF-κB is activated by extracellular or intracellular pathogens, the NF-κB dimer is separated from the IκB protein. The dissociation of the NF-κB dimer from the IκB protein inhibitor results in the translocation of the NF-κB dimer from the cytoplasm into the nucleus, where it binds to DNA and activates the downstream gene transcription of NLRP3 and inflammatory cytokines (54–56). Another upstream process regulating NLRP3 inflammasome is associated with endosomal rupture and the release of cathepsin B (57). In AD, intracellular Aβ fibrils could induce the disruption of phagolysosomes and the activation of the NLRP3 inflammasome upon release of cathepsin B (55, 58).

Based on the aforementioned studies, the NF-κB and cathepsin B pathways were investigated as potential upstream processes associated with **DAPPD**-mediated regulation against NLRP3 inflammasome. First, WT and APP/PS1 mice (7 to 7.5 mo of age) were subject to i.p. administration of vehicle or **DAPPD** at 2 mg/kg/day for 2 mo. Thereafter, the cortices were collected for the gel/Western blot. The cortices from vehicle-treated APP/PS mice showed the elevated levels of pNF-κB p50, pNF-κB p65, and pIκB. Treatment of **DAPPD** reduced the expression of these NF-κB–related proteins. Oppositely, there was no significant difference in the expression of cathepsin B upon administration of **DAPPD** in APP/PS1 mice (Fig. 4*F*). Furthermore, both the NF-κB and cathepsin B pathways were studied in vitro using human microglia treated with Aβ. The in vitro experiments further supported the ability of **DAPPD** to suppress the activation of NF-κB signaling by Aβ. On the other hand, 2 structural analogs of **DAPPD**, *N*,*N*′-(1,4-phenylene)bis(*N*-methylacetamide) (**PBMA**) (2 *N*-methyl groups on **DAPPD**; *SI Appendix*, Fig. S6) and **AAP**, did not noticeably alter the NF-κB signaling and the release of cathepsin B in human microglia (Fig. 5 *A* and *B*). Taken together, our in vivo and in vitro results indicate that **DAPPD** is able to affect the expression of NLRP3 via its impact on the NF-κB pathway.

Improvement of Microglial Dysfunction in Vitro AD Environment by DAPPD. To evaluate the microglial effects of **DAPPD**, we determined the **DAPPD**-mediated regulation of microglial function in vitro employing human microglia. In addition to **DAPPD**, **PBMA** and **AAP** were treated to microglia to investigate their effects as well as a brief structure–activity relationship. Human microglia were incubated with Aβ for 24 h and then were treated with **DAPPD**, **PBMA**, or **AAP** for 24 h. NLRP3 and ASC were up-regulated in human microglia added with Aβ, leading to the increased secretion of cleaved caspase-1 and IL-1β in the supernatant. Treatment of **DAPPD** reduced the production of NLRP3 and ASC and the secretion of cleaved caspase-1 and IL-1β. **PBMA** or **AAP** also induced the down-regulation of cleaved caspase-1 and IL-1β in human microglia; however, the extent of their effects was far weaker than that of **DAPPD** (Fig. 5*A*). Moreover, **DAPPD** suppressed the Aβ-induced activation of NF-κB signaling but not the release of cathepsin B, while **PBMA** or **AAP** did not show these effects (Fig. 5*B*). These observations indicate that **DAPPD** can effectively alter the NF-κB pathway in microglia leading to the down-regulation of NLRP3. Based on the weaker microglial effects induced by **PBMA** and **AAP**, the acetamide groups of **DAPPD** may be important in the molecule's efficacy in restoring microglial function.

Next, the expression of pro- and antiinflammatory cytokines as well as M0-homeostatic and MGnD microglia genes was analyzed in human microglia treated with or without Aβ in the presence of **DAPPD**, **PBMA**, or **AAP**. Aβ-treated human microglia showed up-regulated proinflammatory cytokines and down-regulated antiinflammatory cytokines, while the administration of **DAPPD** restored these changes of inflammatory cytokines (Fig. 5*C*). The expression of M0-homeostatic and MGnD microglia genes also presented similar results (Fig. 5*D*). **PBMA** and **AAP** had less effects on restoration of the abnormal expression of inflammatory and microglia genes by Aβ. These results suggest that **DAPPD** is able to restore neuroinflammation by regulating NLRP3 inflammasome and functional phenotypes of microglia in vitro AD environment. Finally, the impact of **DAPPD** on microglial phagocytosis was verified. Aβ-treated human microglia took noticeably longer to phagocytose fluorescein isothiocyanate (FITC) beads and exhibited an overall reduction in phagocytic capacity, represented by the decrease in the total number of phagocytosed FITC beads (Fig. 5*E* and Movies S1–S8). The treatment of **DAPPD** restored the deficient phagocytic capacity of Aβ-treated human microglia, while human microglia added with **PBMA** and **AAP** did not exhibit these restorative effects on microglial phagocytosis (Fig. 5*E* and Movies S1–S8). Therefore, these results suggest the ability of **DAPPD** to attenuate the microglial dysfunction caused by Aβ.

AAP is known to suppress inflammation by inhibiting the activity of cyclooxygenase 1 (COX-1) or 2 (COX-2) in microglia (26, 59, 60). To further confirm whether the antineuroinflammatory effects of **DAPPD** are a result of its influence on COX, the expression of COX-1 and COX-2 was monitored in microglia upon treatment of **DAPPD**. Aβ was observed to up-regulate the expression of COX-1 and COX-2 in microglia. **AAP** effectively inhibited the Aβ-induced up-regulation of both COX-1 and COX-2. **DAPPD** and **PBMA**, however, had no effect on the expression of COX (*SI Appendix*, Fig. S7). In addition, **DAPPD** showed a very weak inhibitory activity against COX-2 in vitro, with a half maximal inhibitory concentration (IC_{50}) value of 22 ± 1 mM. These results further support that **DAPPD**-mediated restoration of microglial function occurs through the regulation of NLRP3 inflammasome and functional phenotypes of microglia without affecting the expression or activity of COX.

Investigation of DAPPD's Effects toward Aβ Aggregation and Aβ-Degrading Enzymes' Expression. To validate that the reduction of Aβ accumulation, observed in the brains of **DAPPD**-treated AD transgenic mice, was indeed a product of **DAPPD**'s anti-inflammatory activity over direct influence on a decrease in Aβ deposition, the modulating effects of the compound toward the aggregation of $Aβ_{40}$ and $Aβ_{42}$, 2 major isoforms of Aβ (14, 38, 61, 62), and the expression of Aβ-degrading enzymes were probed in vitro and in vivo (WT and APP/PS1 mice), respectively. First, the effects of **DAPPD** toward inhibition of Aβ aggregate formation (inhibition experiment; *SI Appendix*, Fig. S8 *A*, *i*) and

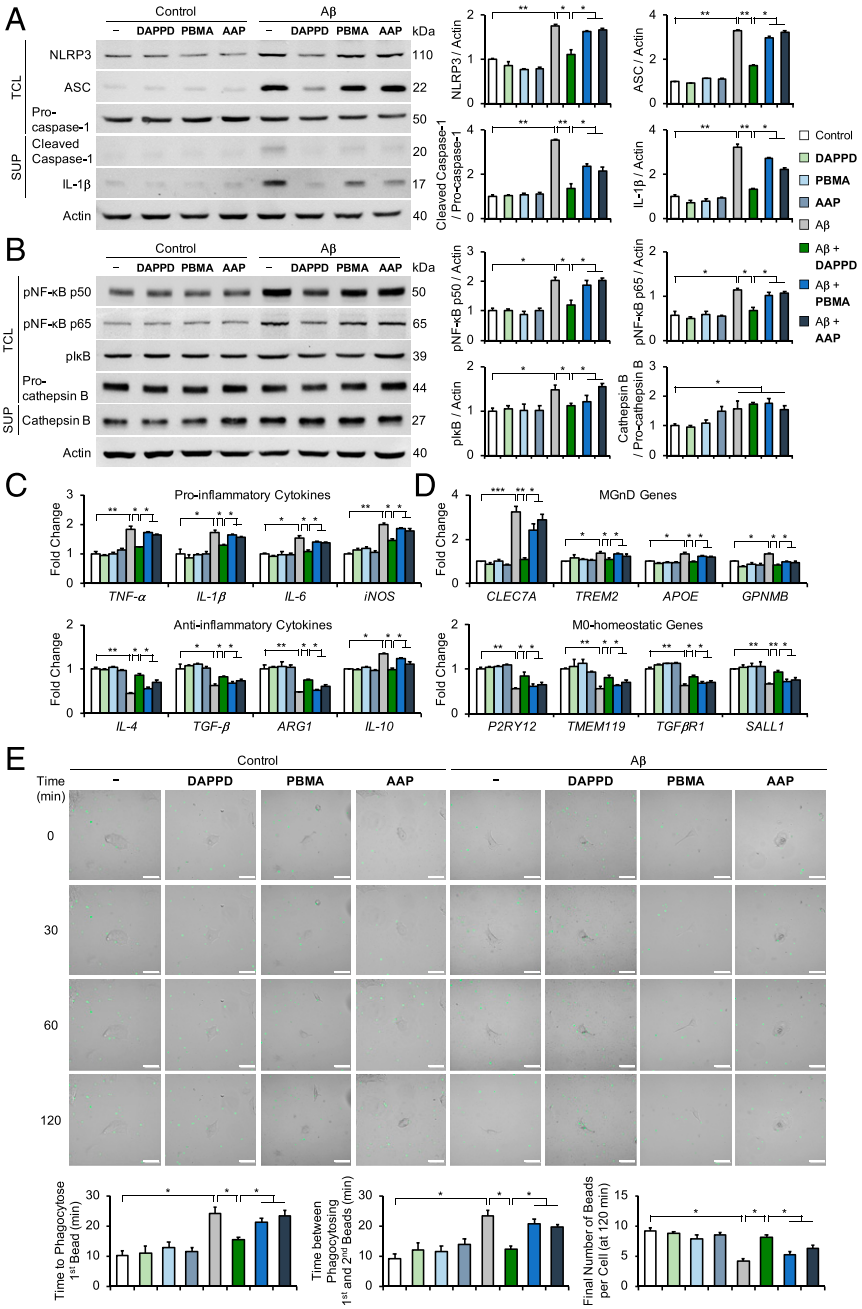

Fig. 5. Effects of **DAPPD**, **PBMA**, and **AAP** on microglial function in vitro AD environment. (*A* and *B*) Impact of **DAPPD**, **PBMA**, and **AAP** on the expression of the proteins related to NLRP3 inflammasome, NF-κB signaling, and cathepsin B in human microglia with and without the addition of Aβ. SUP, supernatant; TCL, total cell lysate. (*C* and *D*) mRNA levels of pro- and antiinflammatory cytokines as well as M0-homeostatic and MGnD microglia genes in human microglia. (*E*, *Top*) Representative images from live-cell imaging at various time points after the administration of FITC beads in each group. (Scale bars, 50 μm.) (*E*, *Bottom*) Analysis of the bead uptake: the amount of time taken to phagocytose the first bead (*Left*), the time between the phagocytosis of the first and second beads (*Middle*), and the final number of beads phagocytosed in 120 min (*Right*) in each group. Animal number: *A*–*D*, $n = 4$ per group; *E*, $n = 6$ per group. $^{*}P < 0.05$; $^{**}P < 0.01$; $^{***}P < 0.001$ by one-way analysis of variance, Tukey's post hoc test. All error bars indicate SEM.

disassembly of preformed Aβ aggregates (disaggregation experiment; *SI Appendix*, Fig. S8 *A*, *ii*) were assessed through gel/Western blot and transmission electron microscopy. In both inhibition and disaggregation experiments, the Aβ species resulted from incubation with **DAPPD** did not indicate noticeable changes in the size distribution and morphology, relative to those generated without **DAPPD** (*SI Appendix*, Fig. S8 *B* and *C*). In short, **DAPPD** does not modify the aggregation of both $Aβ_{40}$ and $Aβ_{42}$, indicative of no significant direct interaction between the compound and Aβ.

Moreover, expression of the enzymes responsible for Aβ degradation (i.e., neprilysin [*Nep*], matrix metallopeptidase 9 [*Mmp9*], and insulin-degrading enzyme [*Ide*]) was analyzed in the brain samples of vehicle- or **DAPPD**-treated APP/PS1 mice. As depicted in *SI Appendix*, Fig. S8*D*, vehicle-treated APP/PS1 mice, compared to vehicle-treated WT mice, indicated the

reduced levels of *Nep*, *Mmp9*, and *Ide*, even with the administration of **DAPPD** (2 mg/kg/day, i.p.; 2 mo; 7.5 mo old). These observations present that **DAPPD** has no effect on the production of Aβ-degrading enzymes. Thus, our studies suggest the restored microglial phagocytic capacity by the treatment of **DAPPD** as the dominant to be responsible for alleviating the accumulation of Aβ species in the brains of AD transgenic mice.

Discussion

Dysfunction of microglia, a pivotal mediator of neuroinflammation, has been increasingly recognized as a causative factor in AD; thus, developing chemical reagents capable of restoring microglial function is critically important and constitutes a promising but underexplored therapeutic strategy. In this work, **DAPPD** was identified as a compact and simple molecule capable of promoting microglial phagocytic function. The activity of **DAPPD** leads to effective attenuation of cognitive deficits in 2 types of AD transgenic mice (i.e., APP/PS1 and 5×FAD mice) and noticeable reduction of Aβ accumulation. Down-regulation of the constituent proteins of NLRP3 inflammasome (i.e., NLRP3 and ASC) through the suppression of the NF-κB pathway, witnessed in the brains of APP/PS1 mice administrated with **DAPPD**, is most likely responsible for the rescue from microglial dysfunction. Our studies confirm that the regulation of neuroinflammation in AD through the rectification of microglial dysfunction using small molecules is a valid therapeutic approach against AD. Furthermore, neuroprotective small molecules capable of recovering microglial dysfunction with subsequent elevation of microglial phagocytic function could also serve as investigative tools to advance our understanding of the role of neuroinflammation in the pathologies of neurodegenerative disorders.

Materials and Methods

All chemical reagents were purchased from commercial suppliers and used as received unless otherwise stated. **DAPPD** and **AAP** were purchased from Alfa Aesar and Sigma-Aldrich. $A\beta_{40}$ (DAEFRHDSGYEVHHQKLVFFAEDVGSNKGAIIGLMVGGVV) and $A\beta_{42}$ (DAEFRHDSGYEVHHQKLVFFAEDVGSNKGAIIGLMVGGVVIA) were purchased from Anaspec or Invitrogen. The buffered solutions were prepared in doubly distilled water (a Milli-Q Direct 16 system [18.2 MΩ·cm; Merck KGaA]). The absorbance values were measured by a SpectraMax M5e microplate reader (Molecular Devices). Metabolic stability assay to predict the half-life and clearance of compounds was evaluated with human liver microsomes (Daegu Gyeongbuk Medical Innovation Foundation). The gel images were recorded on a ChemiDoc MP Imaging System (Bio-Rad). The details of experimental protocols and analytical methods are presented in *SI Appendix*.

ACKNOWLEDGMENTS. This research is supported by National Research Foundation of Korea (NRF) grants funded by the Korean government (NRF-2016R1A5A1009405 and NRF2017R1A2B3002585 [to M.H.L.], NRF-2017R1D1A1B03030567 [to J.-Y.L.], and NRF-2017R1A4A1015652 and NRF-2018M3C7A1056513 [to H.K.J.]); the Korea Advanced Institute of Science and Technology (M.H.L.); the Korea Health Technology Research & Development Project through the Korea Health Industry Development Institute, funded by the Ministry of Health & Welfare, Korea (HI16C2131 [to J.-s.B.]); a National Research Council of Science Technology grant funded by the Korean government (Ministry of Science, ICT and Future Planning) (CAP-17-05-KIGAM [to Y.-H.L.]). We also thank Prof. Su Wol Chung at the University of Ulsan for initial NLRP3-related studies.

1. S. Przedborski, M. Vila, V. Jackson-Lewis, Neurodegeneration: What is it and where are we? *J. Clin. Invest.* **111**, 3–10 (2003).
2. M. T. Heneka *et al.*, Neuroinflammation in Alzheimer's disease. *Lancet Neurol.* **14**, 388–405 (2015).
3. E. C. Hirsch, S. Hunot, Neuroinflammation in Parkinson's disease: A target for neuroprotection? *Lancet Neurol.* **8**, 382–397 (2009).
4. T. Philips, W. Robberecht, Neuroinflammation in amyotrophic lateral sclerosis: Role of glial activation in motor neuron disease. *Lancet Neurol.* **10**, 253–263 (2011).
5. R. M. Ransohoff, How neuroinflammation contributes to neurodegeneration. *Science* **353**, 777–783 (2016).
6. G. W. Kreutzberg, Microglia: A sensor for pathological events in the CNS. *Trends Neurosci.* **19**, 312–318 (1996).
7. F. L. Heppner, R. M. Ransohoff, B. Becher, Immune attack: The role of inflammation in Alzheimer disease. *Nat. Rev. Neurosci.* **16**, 358–372 (2015).
8. U.-K. Hanisch, H. Kettenmann, Microglia: Active sensor and versatile effector cells in the normal and pathologic brain. *Nat. Neurosci.* **10**, 1387–1394 (2007).
9. S. E. Hickman, E. K. Allison, J. El Khoury, Microglial dysfunction and defective β-amyloid clearance pathways in aging Alzheimer's disease mice. *J. Neurosci.* **28**, 8354–8360 (2008).
10. M. L. Block, L. Zecca, J.-S. Hong, Microglia-mediated neurotoxicity: Uncovering the molecular mechanisms. *Nat. Rev. Neurosci.* **8**, 57–69 (2007).
11. E. E. Tuppo, H. R. Arias, The role of inflammation in Alzheimer's disease. *Int. J. Biochem. Cell Biol.* **37**, 289–305 (2005).
12. M. G. Tansey, M. S. Goldberg, Neuroinflammation in Parkinson's disease: Its role in neuronal death and implications for therapeutic intervention. *Neurobiol. Dis.* **37**, 510–518 (2010).
13. M. Prince *et al.*, "World Alzheimer report 2016: Improving healthcare for people living with dementia: Coverage, quality and costs now and in the future" (Alzheimer's Disease International, 2016).
14. M. G. Savelieff *et al.*, Development of multifunctional molecules as potential therapeutic candidates for Alzheimer's disease, Parkinson's disease, and amyotrophic lateral sclerosis in the last decade. *Chem. Rev.* **119**, 1221–1322 (2019).
15. C. Haass, D. J. Selkoe, Soluble protein oligomers in neurodegeneration: Lessons from the Alzheimer's amyloid β-peptide. *Nat. Rev. Mol. Cell Biol.* **8**, 101–112 (2007).
16. J. Y. Lee *et al.*, Neuronal SphK1 acetylates COX2 and contributes to pathogenesis in a model of Alzheimer's Disease. *Nat. Commun.* **9**, 1479 (2018).
17. V. H. Perry, C. Holmes, Microglial priming in neurodegenerative disease. *Nat. Rev. Neurol.* **10**, 217–224 (2014).
18. A. D. Bachstetter *et al.*, Early stage drug treatment that normalizes proinflammatory cytokine production attenuates synaptic dysfunction in a mouse model that exhibits age-dependent progression of Alzheimer's disease-related pathology. *J. Neurosci.* **32**, 10201–10210 (2012).
19. S. Mandrekar-Colucci, J. C. Karlo, G. E. Landreth, Mechanisms underlying the rapid peroxisome proliferator-activated receptor-γ-mediated amyloid clearance and reversal of cognitive deficits in a murine model of Alzheimer's disease. *J. Neurosci.* **32**, 10117–10128 (2012).
20. R. Medeiros *et al.*, Aspirin-triggered lipoxin A4 stimulates alternative activation of microglia and reduces Alzheimer disease-like pathology in mice. *Am. J. Pathol.* **182**, 1780–1789 (2013).
21. Y. Ano *et al.*, Iso-α-acids, bitter components of beer, prevent inflammation and cognitive decline induced in a mouse model of Alzheimer's disease. *J. Biol. Chem.* **292**, 3720–3728 (2017).
22. R. C. Coll *et al.*, A small-molecule inhibitor of the NLRP3 inflammasome for the treatment of inflammatory diseases. *Nat. Med.* **21**, 248–255 (2015).
23. C. Dempsey *et al.*, Inhibiting the NLRP3 inflammasome with MCC950 promotes non-phlogistic clearance of amyloid-β and cognitive function in APP/PS1 mice. *Brain Behav. Immun.* **61**, 306–316 (2017).
24. M. Kim *et al.*, Minimalistic design approach for multi-reactivity against free radicals and metal-free and metal-bound amyloid-β peptides: Redox-based substitutions of benzene. https://doi.org/10.26434/chemrxiv.8051639.v1 (ChemRxiv Preprint, 30 April 2019).
25. E. Sim, A. Abuhammad, A. Ryan, Arylamine *N*-acetyltransferases: From drug metabolism and pharmacogenetics to drug discovery. *Br. J. Pharmacol.* **171**, 2705–2725 (2014).
26. M. Ouellet, M. D. Percival, Mechanism of acetaminophen inhibition of cyclooxygenase isoforms. *Arch. Biochem. Biophys.* **387**, 273–280 (2001).
27. P. J. Amar, E. R. Schiff, Acetaminophen safety and hepatotoxicity–Where do we go from here? *Expert Opin. Drug Saf.* **6**, 341–355 (2007).
28. J. A. Arnott, S. L. Planey, The influence of lipophilicity in drug discovery and design. *Expert Opin. Drug Discov.* **7**, 863–875 (2012).
29. W.-X. Zhao *et al.*, Acetaminophen attenuates lipopolysaccharide-induced cognitive impairment through antioxidant activity. *J. Neuroinflammation* **14**, 17 (2017).
30. J. Rautio *et al.*, Prodrugs: Design and clinical applications. *Nat. Rev. Drug Discov.* **7**, 255–270 (2008).
31. G. Vannuruswamy *et al.*, Molecules with *O*-acetyl group protect protein glycation by acetylating lysine residues. *RSC Adv.* **6**, 65572–65578 (2016).
32. D. R. Howlett *et al.*, Cognitive correlates of Aβ deposition in male and female mice bearing amyloid precursor protein and presenilin-1 mutant transgenes. *Brain Res.* **1017**, 130–136 (2004).
33. H. Oakley *et al.*, Intraneuronal β-amyloid aggregates, neurodegeneration, and neuron loss in transgenic mice with five familial Alzheimer's disease mutations: Potential factors in amyloid plaque formation. *J. Neurosci.* **26**, 10129–10140 (2006).
34. J. S. Derrick *et al.*, A redox-active, compact molecule for cross-linking amyloidogenic peptides into nontoxic, off-pathway aggregates: In vitro and in vivo efficacy and molecular mechanisms. *J. Am. Chem. Soc.* **137**, 14785–14797 (2015).
35. M. W. Beck *et al.*, Structure-mechanism-based engineering of chemical regulators targeting distinct pathological factors in Alzheimer's disease. *Nat. Commun.* **7**, 13115 (2016).
36. L. Mucke, D. J. Selkoe, Neurotoxicity of amyloid β-protein: Synaptic and network dysfunction. *Cold Spring Harb. Perspect. Med.* **2**, a006338 (2012).
37. B. Urbanc *et al.*, Neurotoxic effects of thioflavin S-positive amyloid deposits in transgenic mice and Alzheimer's disease. *Proc. Natl. Acad. Sci. U.S.A.* **99**, 13990–13995 (2002).
38. S. J. C. Lee, E. Nam, H. J. Lee, M. G. Savelieff, M. H. Lim, Towards an understanding of amyloid-β oligomers: Characterization, toxicity mechanisms, and inhibitors. *Chem. Soc. Rev.* **46**, 310–323 (2017).

39. P. Dowling, M. Clynes, Conditioned media from cell lines: A complementary model to clinical specimens for the discovery of disease-specific biomarkers. *Proteomics* **11**, 794–804 (2011).
40. K. Biber, H. Neumann, K. Inoue, H. W. Boddeke, Neuronal 'On' and 'Off' signals control microglia. *Trends Neurosci.* **30**, 596–602 (2007).
41. S. E. Hickman *et al*., The microglial sensome revealed by direct RNA sequencing. *Nat. Neurosci.* **16**, 1896–1905 (2013).
42. O. Butovsky *et al*., Identification of a unique TGF-β-dependent molecular and functional signature in microglia. *Nat. Neurosci.* **17**, 131–143 (2014).
43. I. R. Holtman *et al*., Induction of a common microglia gene expression signature by aging and neurodegenerative conditions: A co-expression meta-analysis. *Acta Neuropathol. Commun.* **3**, 31 (2015).
44. H. Keren-Shaul *et al*., A unique microglia type associated with restricting development of Alzheimer's disease. *Cell* **169**, 1276–1290.e17 (2017).
45. S. Krasemann *et al*., The TREM2-APOE pathway drives the transcriptional phenotype of dysfunctional microglia in neurodegenerative diseases. *Immunity* **47**, 566–581.e9 (2017).
46. M.-V. Guillot-Sestier *et al*., Il10 deficiency rebalances innate immunity to mitigate Alzheimer-like pathology. *Neuron* **85**, 534–548 (2015).
47. A. Karperien, H. Ahammer, H. F. Jelinek, Quantitating the subtleties of microglial morphology with fractal analysis. *Front. Cell. Neurosci.* **7**, 3 (2013).
48. G. Krabbe *et al*., Functional impairment of microglia coincides with β-amyloid deposition in mice with Alzheimer-like pathology. *PLoS One* **8**, e60921 (2013).
49. M. T. Heneka *et al*., NLRP3 is activated in Alzheimer's disease and contributes to pathology in APP/PS1 mice. *Nature* **493**, 674–678 (2013).
50. F. G. Bauernfeind *et al*., Cutting edge: NF-kappaB activating pattern recognition and cytokine receptors license NLRP3 inflammasome activation by regulating NLRP3 expression. *J. Immunol.* **183**, 787–791 (2009).
51. S. G. Boaru *et al*., NLRP3 inflammasome expression is driven by NF-κB in cultured hepatocytes. *Biochem. Biophys. Res. Commun.* **458**, 700–706 (2015).
52. T. Lawrence, The nuclear factor NF-kappaB pathway in inflammation. *Cold Spring Harb. Perspect. Biol.* **1**, a001651 (2009).
53. A. Oeckinghaus, S. Ghosh, The NF-kappaB family of transcription factors and its regulation. *Cold Spring Harb. Perspect. Biol.* **1**, a000034 (2009).
54. P. K. Anand, R. K. S. Malireddi, T.-D. Kanneganti, Role of the nlrp3 inflammasome in microbial infection. *Front. Microbiol.* **2**, 12 (2011).
55. H. Guo, J. B. Callaway, J. P. Ting, Inflammasomes: Mechanism of action, role in disease, and therapeutics. *Nat. Med.* **21**, 677–687 (2015).
56. M. S. J. Mangan *et al*., Targeting the NLRP3 inflammasome in inflammatory diseases. *Nat. Rev. Drug Discov.* **17**, 588–606 (2018).
57. A. Halle *et al*., The NALP3 inflammasome is involved in the innate immune response to amyloid-β. *Nat. Immunol.* **9**, 857–865 (2008).
58. V. Y. H. Hook, M. Kindy, G. Hook, Inhibitors of cathepsin B improve memory and reduce β-amyloid in transgenic Alzheimer disease mice expressing the wild-type, but not the Swedish mutant, β-secretase site of the amyloid precursor protein. *J. Biol. Chem.* **283**, 7745–7753 (2008).
59. S. W. Saliba *et al*., AM404, paracetamol metabolite, prevents prostaglandin synthesis in activated microglia by inhibiting COX activity. *J. Neuroinflammation* **14**, 246 (2017).
60. W. T. Slattery, A. Klegeris, Acetaminophen metabolites *p*-aminophenol and AM404 inhibit microglial activation. *Neuroimmunol. Neuroinflamm.* **5**, 11 (2018).
61. I. W. Hamley, The amyloid beta peptide: A chemist's perspective. Role in Alzheimer's and fibrillization. *Chem. Rev.* **112**, 5147–5192 (2012).
62. A. S. DeToma, S. Salamekh, A. Ramamoorthy, M. H. Lim, Misfolded proteins in Alzheimer's disease and type II diabetes. *Chem. Soc. Rev.* **41**, 608–621 (2012).